Climate Projections Very Likely Underestimate Future Volcanic Forcing and its Climatic Effects

Man Mei Chim[1], Thomas J. Aubry[2], Nathan Luke Abraham[1,3], Lauren Marshall[4], Jane Mulcahy[5], Jeremy Walton[5], Anja Schmidt[1,6,7]

[1] Centre for Atmospheric Science, Yusuf Hamied Department of Chemistry, University of Cambridge, Cambridge, United Kingdom
[2] Department of Earth and Environmental Sciences, University of Exeter, Penryn, United Kingdom
[3] National Centre for Atmospheric Science, United Kingdom
[4] Department of Earth Sciences, Durham University, Durham, United Kingdom
[5] Met Office, FitzRoy Road, Exeter, United Kingdom
[6] German Aerospace Center (DLR), Institute of Atmospheric Physics (IPA), Oberpfaffenhofen, Germany
[7] Ludwig-Maximilians University Munich, Meteorological Institute, Munich, Germany

Corresponding author: Man Mei Chim (mmc70@cam.ac.uk)

Key Points:

- There is a 95% chance that the time-averaged 2015-2100 volcanic SO_2 flux from explosive eruptions exceeds the time-averaged 1850-2014 flux
- Standard climate projections very likely underestimate the 2015-2100 stratospheric aerosol optical depth and volcanic climate effects
- Small-magnitude eruptions (< 3 Tg SO_2) contribute 30% to 50% of the volcanic climate effects in a median future eruption scenario

Abstract

Standard climate projections represent future volcanic eruptions by a constant forcing inferred from 1850-2014 volcanic forcing. Using the latest ice-core and satellite records to design stochastic eruption scenarios, we show that there is a 95% probability that explosive eruptions could emit more sulfur dioxide (SO_2) into the stratosphere over 2015-2100 than current standard climate projections (i.e., ScenarioMIP). Our simulations using the UK Earth System Model with interactive stratospheric aerosols show that for a median future eruption scenario, the 2015-2100 average global-mean stratospheric aerosol optical depth (SAOD) is double that used in ScenarioMIP, with small-magnitude eruptions (< 3 Tg of SO_2) contributing 50% to SAOD perturbations. We show that volcanic effects on large-scale climate indicators, including global surface temperature, sea level and sea ice extent, are underestimated in ScenarioMIP because current climate projections do not fully account for the recurrent frequency of volcanic eruptions of different magnitudes.

Plain Language Summary

Climate projections are the simulations of Earth's climate in the future using complex climate models. Standard climate projections, as in Intergovernmental Panel on Climate Change Sixth Assessment Report, assume that explosive volcanic activity over 2015-2100 are of the same level as the 1850-2014 period. Using the latest ice-core and satellite records, we find that explosive eruptions could emit more sulfur dioxide into the upper atmosphere for the period of 2015-2100 than standard climate projections. Our climate model simulations show that the impacts of volcanic eruptions on climate, including global surface temperature, sea level and sea ice extent, are underestimated because current climate projections do not fully account for the recurrent frequency of volcanic eruptions. We also find that small-magnitude eruptions occur frequently and can contribute a significant effect on future climate.

1. Introduction

Large explosive volcanic eruptions can inject sulfur dioxide (SO_2) forming volcanic sulfate aerosols in the stratosphere that scatter incoming solar radiation, resulting in negative radiative forcing and global surface cooling for 1-3 years (McCormick et al., 1995). Stratospheric volcanic sulfate aerosols also heat the stratosphere by absorbing infrared and near-infrared radiation, which can further induce complex climate responses on seasonal to multi-decadal timescales (see Marshall et al. (2022) for a review).

As we cannot predict future volcanic eruptions, a constant volcanic forcing is commonly used in climate projections, e.g., as done in Phase 6 of the Coupled Model Intercomparison Project (CMIP6; Eyring et al., 2016), which informs the Intergovernmental Panel on Climate Change (IPCC) Sixth Assessment Report. In the CMIP6 Scenario MIP (ScenarioMIP; O'Neill et al., 2016), the constant volcanic forcing is inferred from the time average of the reconstructed 1850-2014 volcanic forcing. This approach does not account for how the sporadic occurrence of volcanic eruptions may affect the climate as opposed to a time-averaged forcing. In addition, volcanic injections into the stratosphere during the Holocene (past 11,500 years; Sigl et al.,

76   2022) can vary by as much as a factor of 25 on centennial timescales. The corresponding
77   uncertainty on future volcanic forcing is currently unaccounted for in most climate projections. A
78   handful of studies have attempted to quantify the role of volcanic forcing uncertainty in climate
79   projections (Ammann and Naveau, 2010; Bethke et al., 2017; Dogar et al., 2020). Bethke et al.
80   (2017) estimated the volcanic forcing of 60 different future eruption scenarios from 2015 to 2100
81   by resampling ice-core sulfate deposition records going back 2,500 years (Sigl et al., 2015). Up-
82   to-date ice-core and satellite volcanic sulfur emission datasets enable us to account for the
83   occurrence of (i) eruptions larger in magnitude than those that occurred between 1850 and 2014,
84   which injected as much as 300 Tg of SO_2 into the atmosphere, and (ii) small-magnitude
85   eruptions below the detection threshold of ice-core datasets (Figure 1a), which can contribute a
86   significant fraction to stratospheric aerosol optical depth (SAOD) (Santer et al., 2014; Schmidt et
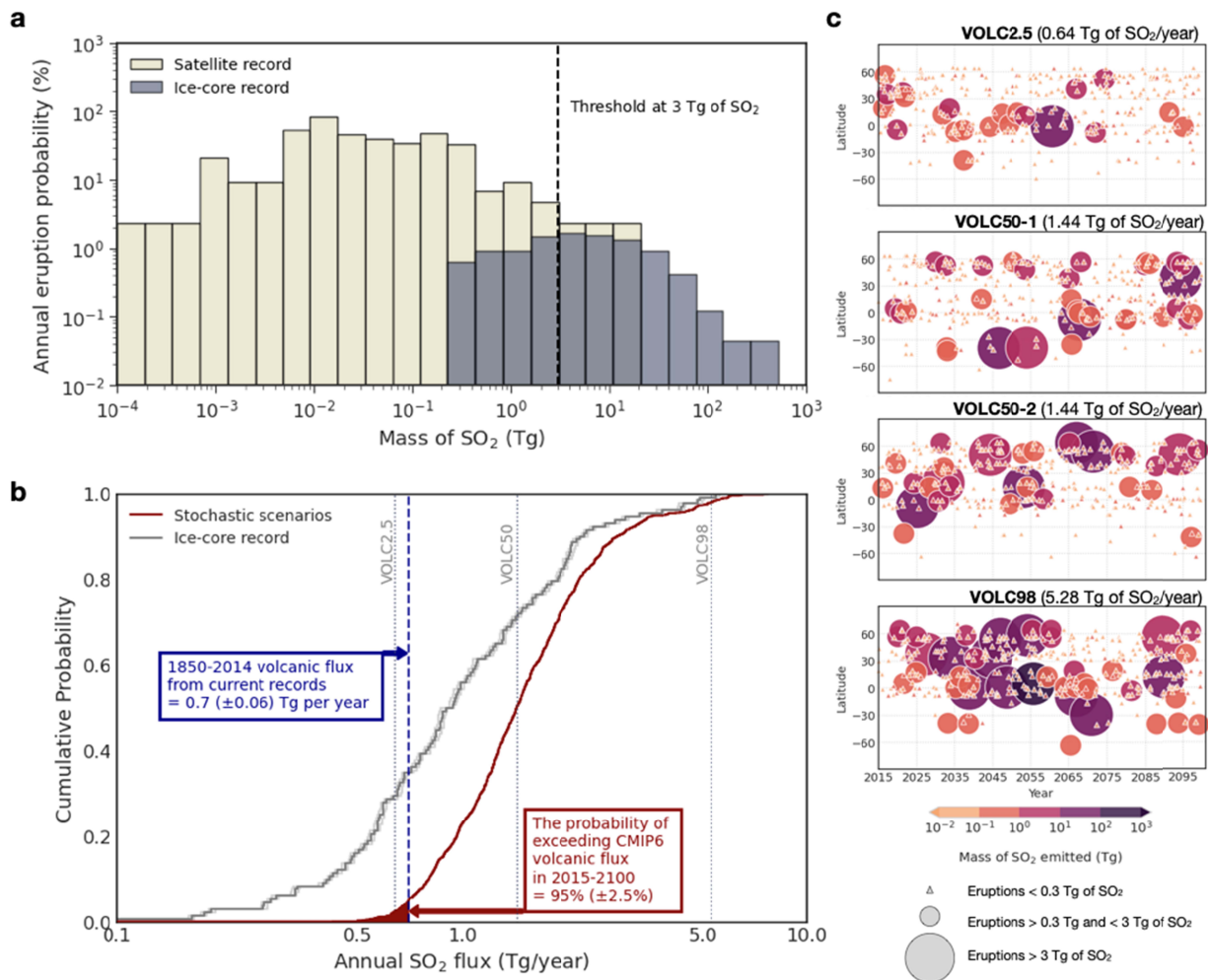87   al., 2018).
88

89
90   **Figure 1**. (**a**) Annual eruption probability based on ice-core (Sigl et al., 2022) and satellite (Carn
91   et al., 2022) datasets. (**b**) Empirical cumulative probability density function of the SO_2 mass
92   distribution of the 1000-member stochastic scenarios and the Holvol ice-core dataset (with 95%
93   bootstrap confidence bounds, in light grey). We estimate the probability of exceeding CMIP6
94   volcanic flux using the 1850-2014 flux from current volcanic SO_2 emission records (Neely and

95   Schmidt, 2016; Sigl et al., 2022; Carn, 2022). (**c**) Eruption time series of VOLC2.5, VOLC50-1,
96   VOLC50-2, and VOLC98 with annual volcanic SO_2 flux of each scenario in brackets.

97

98   In addition, whether they apply a constant volcanic forcing (e.g., CMIP6 ScenarioMIP) or
99   use stochastic eruption scenarios (Bethke et al., 2017), existing climate projections use
100   prescribed volcanic aerosol optical properties derived from simplified volcanic aerosol models.
101   Climate models with interactive stratospheric aerosols (Timmreck et al., 2018) showed a better
102   agreement between the simulated surface temperature responses and tree-ring surface
103   temperature reconstructions for the 1257 Mount Samalas and 1815 Mount Tambora eruptions
104   (Stoffel et al., 2015) and the 1783-1784 Laki eruption (Pausata et al., 2015; Zambri et al., 2019).
105   Furthermore, the prescribed aerosol approach cannot account for the impacts of global warming
106   on the life cycle of volcanic sulfate aerosols (Aubry et al., 2021), including the impact of
107   changing atmospheric stratification on volcanic plume height (Aubry et al., 2019). Such climate-
108   volcano feedbacks might amplify the peak global-mean radiative forcing associated with large-
109   magnitude tropical eruptions by 30% (Aubry et al., 2021).

110

111   Our study aims to improve our understanding of future volcanic impacts on climate. To
112   this end, we perform model simulations from 2015 to 2100 with two innovations: (i) a stochastic
113   resampling approach using the latest ice-core and satellite datasets to generate improved future
114   volcanic eruption scenarios; and (ii) a plume-aerosol-chemistry-climate modeling framework
115   (named UKESM-VPLUME), which combines a volcanic plume model and an Earth System
116   Model with interactive stratospheric aerosols to simulate volcanic climate effects while
117   accounting for climatic controls on plume-rise height.

118

119 **2. Methodology**

120

121   2.1 Stochastic future eruption scenarios

122

123   We generate 1000 stochastic future eruption scenarios for 2015 to 2100 by resampling
124   SO_2 mass from volcanic emission inventories from a bipolar ice-core array covering the past
125   11,500 years (Holvol; Sigl et al., 2022) and a multi-satellite record from 1979 to 2021 (Carn et
126   al., 2016; Carn, 2022) (Figure 1a and S1). Before resampling, we filter out: i) effusive eruptions;
127   ii) in the satellite record, eruptions with eruptive plume heights more than 3 km below the
128   thermal tropopause (obtained from NCEP/NCAR Reanalysis 1; Kalnay et al., 1996); we assume
129   that aerosol lofting could result in stratospheric injections for tropospheric plumes less than 3 km
130   below the tropopause. By examining the eruption frequency-magnitude (i.e., in this study, SO_2
131   mass) distribution of both ice-core and satellite records (Figure 1a), we identify 3 Tg of SO_2 as a
132   threshold: i) below which ice-core records underestimate eruption frequency due to under-
133   recording; and ii) above which the short duration of the satellite record precludes it from
134   capturing the true frequency of eruptions with higher magnitude. Accordingly, we use a 3 Tg of
135   SO_2 threshold to define "small-magnitude" and "large-magnitude" eruptions. We resample
136   small-magnitude eruptions from the satellite record only, and large-magnitude ones from the
137   combined ice-core and satellite record. Details of the resampling of the erupting volcano, SO_2
138   mass, and mass eruption rate are discussed in the Supplementary Information.

139

140

141   2.2 UKESM-VPLUME

143   Atmospheric stratification, wind and humidity affect volcanic plume dynamics and SO_2
144 injection height (e.g., Mastin, 2014), but SO_2 height is commonly prescribed in modelling studies
145 of volcanic forcing (e.g., Timmreck et al., 2018). To account for meteorological controls on
146 plume dynamics, we have developed UKESM-VPLUME, which couples the UK Earth System
147 Model (UKESM; Mulcahy et al., 2023) with Plumeria (1-D eruptive plume model; Mastin, 2007,
148 2014) (details in Supplementary Information). We use version 1.1 of UKESM with fully-coupled
149 atmosphere-land-ocean and interactive stratospheric aerosols. In brief, for each time step of the
150 UKESM atmospheric model during an eruption, UKESM-VPLUME interactively passes the
151 atmospheric conditions simulated at the eruption location to Plumeria. Plumeria then computes
152 the neutral buoyancy height of the volcanic plume based on atmospheric conditions and the mass
153 eruption rate generated for each eruption in the stochastic scenarios. Volcanic SO_2 is injected
154 into UKESM at the neutral buoyancy height calculated in Plumeria using a gaussian profile with
155 a width of 10% of the plume height (consistent with large-eddy simulations of volcanic plumes,
156 Aubry et al., 2019). This approach ensures that plume heights of volcanic eruptions are
157 consistent with the meteorological conditions simulated by UKESM.

159   2.3 Experimental design

161   We perform simulations using the UKESM-VPLUME framework for four stochastic
162 future eruption scenarios at the 2.5^{th}, 50.0^{th}, 50.5^{th} and 98.0^{th} percentiles (termed VOLC2.5,
163 VOLC50-1, VOLC50-2, VOLC98) of the distribution of the 2015-2100 average SO_2 flux across
164 the 1000 future eruption scenarios (Figure 1b). We choose scenarios close (within 0.5 percentile)
165 to the 2.5^{th}, 50th and 97.5^{th} to sample the median and 95% confidence interval of the future
166 volcanic stratospheric SO_2 injections. To test future climate trajectory sensitivity to the temporal
167 and spatial distribution of eruptions, we run two scenarios near the 50th percentile. For instance,
168 VOLC50-2 has more large-magnitude eruptions than VOLC50-1 in the early 21st century (Figure
169 1c). We also performed the VOLC50 runs with small-magnitude eruptions only (VOLC50-1S
170 and VOLC50-2S) to isolate their contribution to the overall climate effects caused by eruptions
171 of all magnitudes. We compare the results from VOLC runs with runs without volcanic eruptions
172 (NOVOLC) and with CMIP6 ScenarioMIP constant volcanic forcing (CONST). We perform all
173 simulations from 2015 to 2100 under a high-end future emission scenario (SSP3-7.0 in
174 ScenarioMIP) running three ensemble members for each scenario.

176 **3. Results**

177   Figure 2 shows the global monthly-mean SAOD at 550 nm and the time-averaged values
178 over 2015-2100. The time-averaged ensemble-mean SAOD ranges from 0.015 ± 0.0004
179 (VOLC2.5) to 0.062 ± 0.0018 (VOLC98), with an average value of 0.024 ± 0.0012 for the two
180 median future eruption scenarios (VOLC50), while the SAOD in CONST, which followed the
181 ScenarioMIP design, is 0.012 ± 0.0018 (one standard deviation uncertainty). Small-magnitude
182 eruptions contribute 0.010 to 0.013 ± 0.0002 to the time-averaged SAOD in the VOLC50
183 scenarios, i.e., about 50% of the total SAOD. Comparing VOLC2.5 to CONST and assuming
184 that the rank for the 2015-2100-year mean volcanic SO_2 flux and SAOD are the same, it is thus
185 very likely (i.e., > 90% probability following IPCC guidance note; Mastrandrea et al., 2010) that

186 the actual global 2015-2100 mean SAOD will be higher than that prescribed in ScenarioMIP,
187 with the median (VOLC50) SAOD value being double that used in ScenarioMIP. The result is
188 consistent with Figure 1, given that the 1850-2014 time-averaged SO_2 flux used to define the
189 ScenarioMIP volcanic forcing is close to the 2.5[th] percentile of the future volcanic SO_2 flux
190 distribution. Beyond the time-averaged SAOD value, owing to the sporadic nature of volcanic
191 eruptions, the global monthly-mean SAOD values in VOLC scenarios can be up to a factor of 60
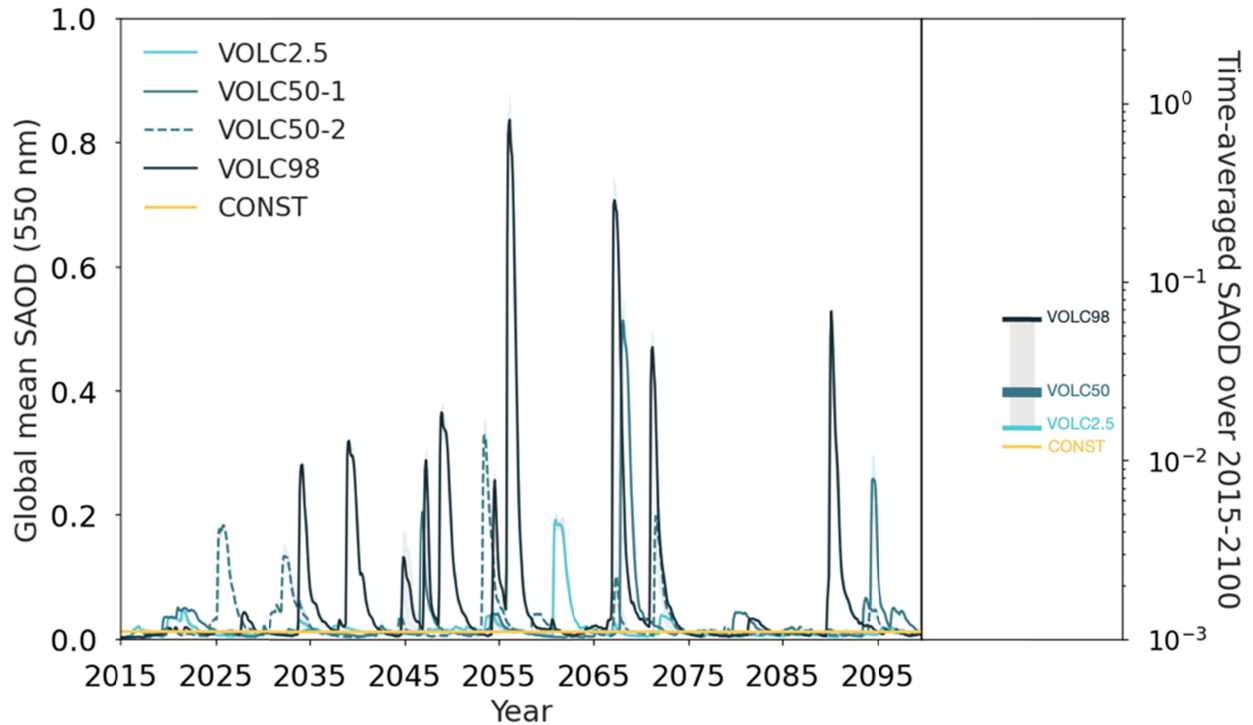192 greater than that in ScenarioMIP (Figures 2 and S2).

193
194 **Figure 2**. (Left) Global monthly-mean SAOD at 550 nm. The lines show the ensemble mean and
195 the shading shows the spread of the maximum and minimum ensemble members. (Right) The
196 corresponding time-averaged SAOD over 2015-2100 (in log scale).

197   Figure 3a shows the global annual-mean surface air temperature at 1.5 m (GMST)
198 relative to the 1850-1900 period. Large-magnitude volcanic eruptions lead to a short-term drop
199 in the annual-mean GMST for at least 1 year and up to 6 to 7 years for the largest eruptions. In
200 the VOLC98 scenario where clusters of large-magnitude eruptions occur, they can induce multi-
201 decadal global cooling. The 2015-2100 time-averaged GMST relative to detrended NOVOLC
202 ensemble mean (Figure 3b) ranges between -0.16 ºC (VOLC2.5) and -0.56 ºC (VOLC98), with
203 CONST lying outside this range at -0.12 ºC. Volcanic cooling for median eruption scenarios
204 (VOLC50-1 and VOLC50-2) is 0.20 to 0.24 ºC, double that of CONST, and 0.09 to 0.10 ºC of
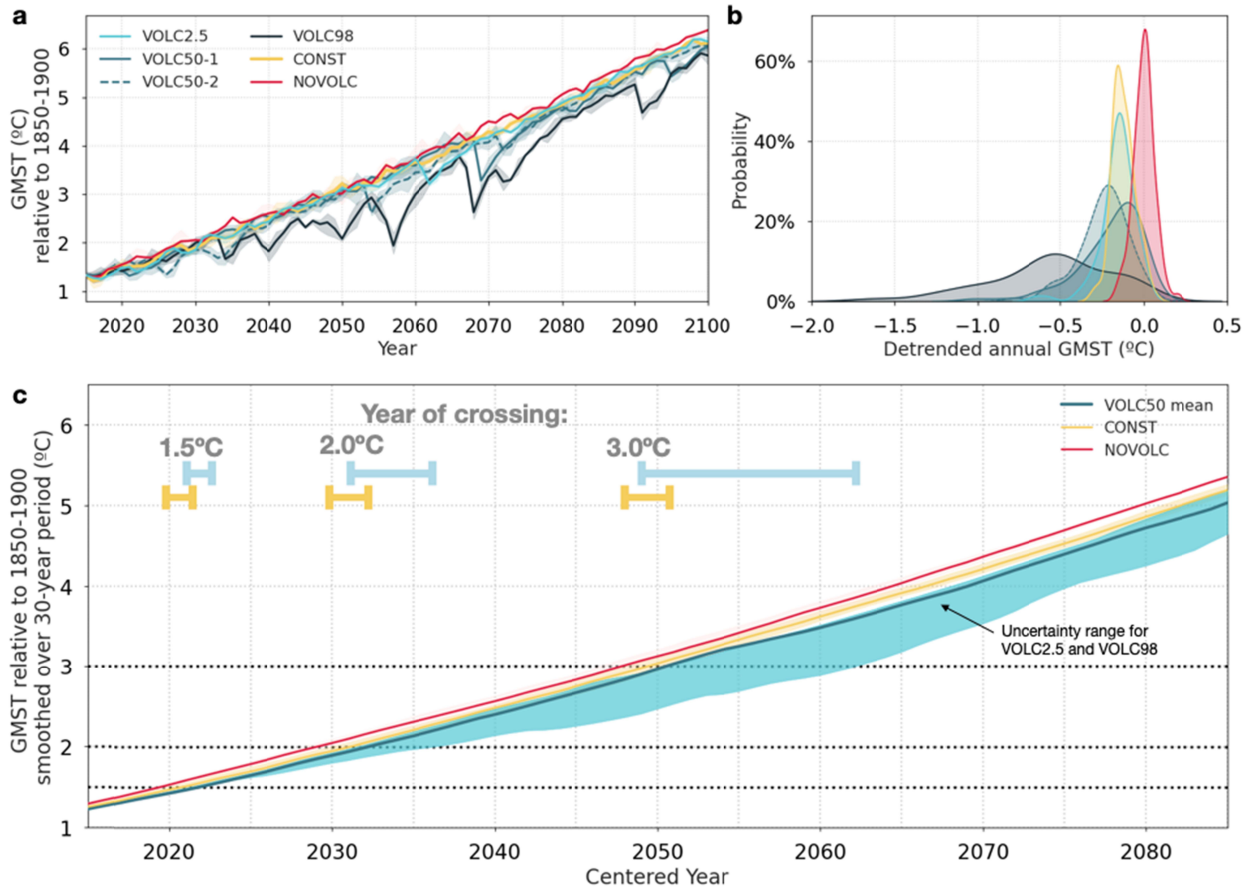205 cooling is attributable to small-magnitude eruptions (Table S1).

206

Figure 3. (**a**) Annual-mean GMST relative to 1850-1900. The lines show the ensemble mean and the shading shows the spread of the maximum and minimum ensemble members. (**b**) Probability density function of the annual-mean GMST relative to detrended NOVOLC ensemble mean (see Supplementary Information). (**c**) 30-year moving mean GMST with years of crossing 1.5 ºC, 2 ºC, and 3 ºC for VOLC and CONST runs.

The IPCC defines global warming as an increase, relative to 1850-1900, in the global mean surface air and sea surface temperatures over a period of 30 years (IPCC, 2021). Using this definition, we examine the year of crossing of 1.5 ºC, 2 ºC, and 3 ºC warming thresholds for VOLC and CONST runs (Figure 3c). Volcanic eruptions delay the time of crossing 1.5 ºC by about 1.6 to 3.2 years when compared to NOVOLC (Table S2), consistent with Bethke et al. (2017). Compared to CONST, times of temperature threshold crossings are significantly delayed by 1.8 to 2.5 years in VOLC50-2, but unaffected in VOLC50-1. This highlights the sensitivity of the time of crossing to the temporal distribution of large-magnitude eruptions. The occurrence of volcanic clusters in VOLC98 causes an extended cooling period between 2034 to 2060 (Figure 3a) which delays the crossing of 2 ºC and 3 ºC by 7 and 14 years, respectively.

In Figure 4, we examine volcanic effects on large-scale climate indicators other than GMST. The 2015-2100 time-averaged global annual-mean precipitation fluxes in all VOLC runs show a greater reduction than CONST, with a range between -0.014 mm/day (VOLC2.5) to -0.052 mm/day (VOLC98), and -0.010 mm/day for CONST (Figure 4a). In VOLC50 scenarios,

228   the global annual-mean precipitation flux is reduced by 0.019 mm/day with small-magnitude

229   eruptions alone contributing between 0.008 and 0.009 mm/day, comparable to the effects of the

230   volcanic forcing implemented in ScenarioMIP. It is thus very likely that the reduction of global

231   mean precipitation due to volcanic effects is underestimated in ScenarioMIP.
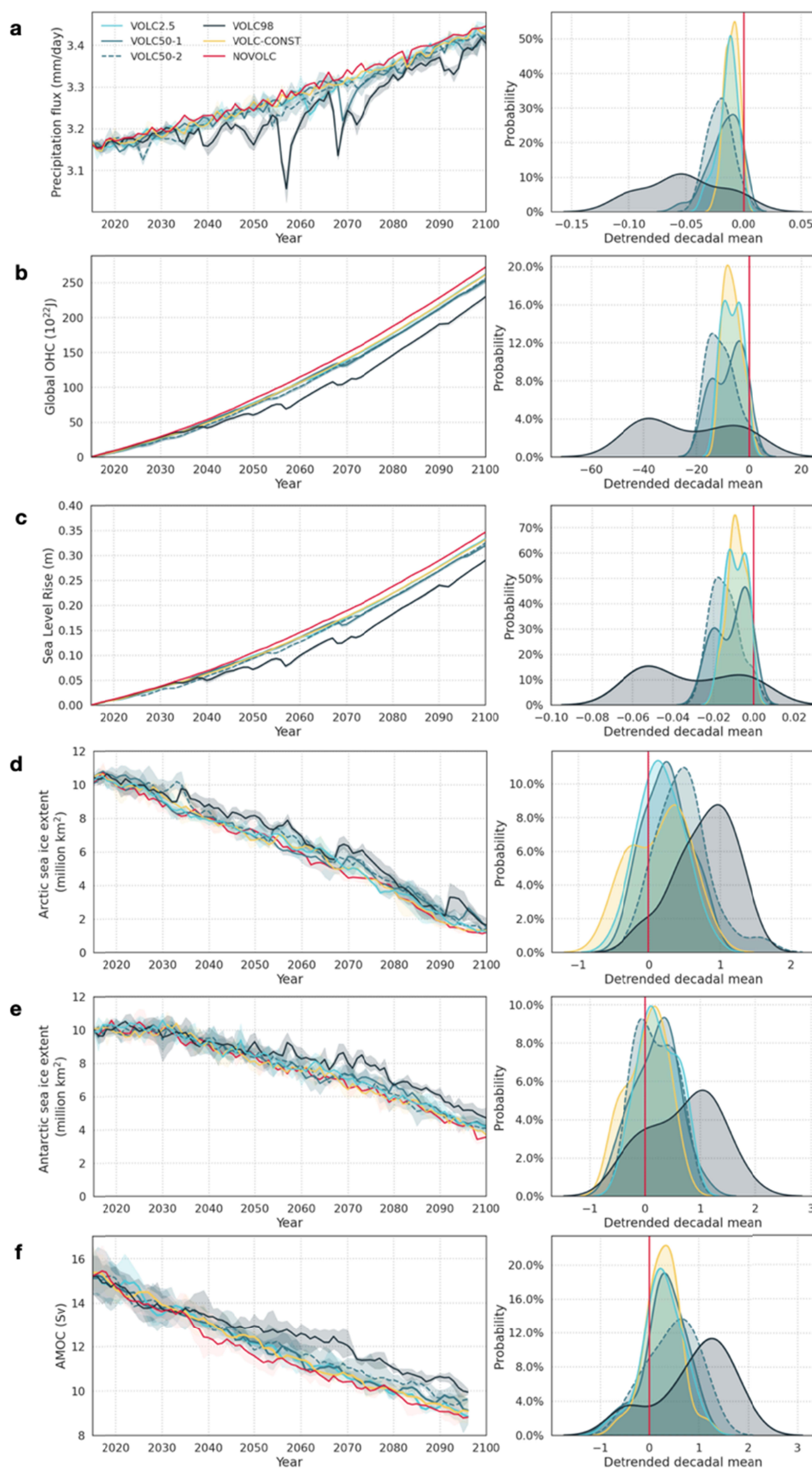
233
234 **Figure 4**. (Left) Annual mean time series of selected large-scale climate indicators. The line
235 shows the ensemble mean and the shading shows the spread of the maximum and minimum
236 ensemble members. (Right) The corresponding decadal-mean probability density function
237 relative to the detrended NOVOLC ensemble mean, with the red vertical line showing the mean
238 of NOVOLC. (**a**) global precipitation flux (in mm/day), (**b**) global ocean heat content (in 10^{22} J),
239 (**c**) global thermosteric sea level rise (in m), (**d** and **e**) Arctic and Antarctic sea ice extent (in
240 million km^2), defined as the area with >15% sea ice, (f) 5-year moving mean AMOC at 26ºN (in
241 Sv).

242   Volcanic-induced surface cooling penetrates into the deep ocean layer and decreases the
243 global ocean heat content (Figures 4b and S3), which in turn leads to less thermal expansion in
244 seawater and a reduction in thermosteric sea level (Figure 4c). Volcanic forcing in VOLC50
245 reduces global ocean heat content and thermosteric sea level by 6% to 7% compared to
246 NOVOLC by 2100, whereby about half is attributed to small-magnitude eruptions (Figure S3).
247 Although volcanic forcing can cause considerable impacts on large-scale ocean metrics, it does
248 not offset the anthropogenic-induced ocean warming trends even for the upper-end volcanic
249 emission scenario VOLC98 (Figures 4b, 4c and 4f).

250   Depending on the eruption magnitude and location, the Arctic and Antarctic sea ice
251 extents show an immediate increase for 1-2 years after large-magnitude eruptions (Figures 4d
252 and 4e). The time-averaged global sea ice extent in VOLC runs over 2015 to 2100 increases by
253 0.43 million km^2 (VOLC2.5) to 1.53 million km^2 (VOLC98) as compared to 0.20 million km^2
254 for CONST. Comparing VOLC2.5 to CONST suggests that for similar time-averaged SAOD, the
255 use of a constant forcing instead of a stochastic eruption distribution halves the magnitude of the
256 sea ice response.

257   The time-averaged Atlantic Meridional Overturning Circulation (AMOC) at 26ºN over
258 2015 to 2100 is strengthened by between 0.26 Sv (VOLC2.5) and 0.93 Sv (VOLC98) as
259 compared to NOVOLC, with all VOLC scenarios exhibiting an increased decadal mean AMOC
260 strength (Figure 4f). The stronger AMOC responses in VOLC runs are consistent with reduced
261 precipitation over the Northern Hemisphere, which increases salinity and enhances deep-water
262 formation (Pausata et al., 2015). Small-magnitude eruptions alone can increase the time-averaged
263 AMOC strength by 0.36-0.38 Sv (VOLC50-1S and VOLC50-2S), which is greater than CONST
264 at 0.28 Sv, and contribute to over 77% of the AMOC response in the median future scenarios
265 (Table S1). One of the median future scenarios (VOLC50-1) has a weaker time-averaged AMOC
266 than the same run with small-magnitude eruptions only (VOLC50-1S) due to an extended period
267 of weakened AMOC after the occurrence of large-magnitude eruptions (Figure S4), suggesting
268 AMOC may have different responses towards different latitudinal and SO$_2$ distributions of large-
269 magnitude eruptions.

270 **4. Discussion**
271
272   Small-magnitude eruptions (< 3 Tg of SO$_2$) contribute a considerable fraction (between
273 33% and 40%) of the total upper atmospheric volcanic SO$_2$ emissions in VOLC50, and in turn,
274 are responsible for 30% to 50% of the volcanic impact on selected large-scale climate indicators
275 and over 77% of the AMOC response (Figure 5 and Table S1). For future eruption scenarios

276 with fewer eruptions than VOLC50, the contribution from small-magnitude eruptions is expected
277 to be even greater because the total mass injected by small-magnitude eruptions is relatively
278 similar across all scenarios. Despite the importance of volcanic forcing from small-magnitude
279 eruptions, they are mostly unaccounted for in historical simulations before satellite
280 measurements are available. In the pre-satellite historical period (1850-1978), the Neely and
281 Schmidt (2016) and Sigl et al. (2022) volcanic SO_2 inventories have an average flux of 0.21 and
282 0.26 Tg of SO_2 per year from small-magnitude eruptions, respectively. By comparison, the flux
283 is 0.50 Tg of SO_2 per year over 1979-2021 (Carn, 2022). This suggests a missing flux from
284 small-magnitude eruptions of between 0.24 and 0.29 Tg of SO_2 per year in the pre-satellite
285 historical period, which is the equivalent of injections from about 1 to 2 Mount Pinatubo 1991
286 eruptions.
287
288 Our stochastic scenarios imply that CMIP6 ScenarioMIP very likely (95 ± 2.5%)
289 underestimates the 2015-2100 volcanic SO_2 flux from explosive eruptions and, in turn, forcing
290 (Figure 1b). Figure 1b shows the cumulative probability against the annual SO_2 flux obtained by
291 resampling ice-core record of volcanic SO_2 injection only (i.e., Holvol; Sigl et al. 2022) and both
292 ice-core and satellite (Carn, 2022) records as in our stochastic scenarios. CMIP6 ScenarioMIP
293 uses a constant volcanic forcing inferred from the 1850-2014 period during which the mean
294 volcanic SO_2 flux recorded in emission inventories was 0.7 ± 0.06 Tg per year. However, we find
295 a 95% confidence interval for the 2015-2100 mean volcanic SO_2 flux between 0.64 to 5.28 Tg
296 per year in our eruption scenarios (Figure 1b). Our stochastic approach, which represents better
297 the frequency-magnitude distribution of small-magnitude eruptions, results in a higher annual
298 SO_2 flux than resampling from the ice-core record only (e.g., Bethke et al., 2017).
299
300 Our future volcanic eruption scenarios greatly enhance the variability of large-scale
301 climate indicators as compared to the ScenarioMIP forcing (Figure 5). Future volcanic emissions
302 in our scenarios cause a 3.5% (VOLC2.5) to 15.0% (VOLC98) decrease in the 2015-2100 time-
303 averaged global net radiative forcing at the top-of-the-atmosphere relative to the anthropogenic
304 contribution (Figures 5 and S5, see Supplementary Information). The time-averaged climate
305 responses of our selected climate indicators scale with the magnitude of volcanic forcing except
306 for the Antarctic sea ice extent and AMOC, which may depend on the latitudinal distribution of
307 eruptions. We also find that the magnitude of volcanic effects on climate indicators are
308 comparable between CONST and VOLC2.5, which is a scenario with only one Pinatubo-like
309 eruption over 2015-2100. Our results suggest that due to the low volcanic forcing used in
310 ScenarioMIP, it is very likely (97.5%) that ScenarioMIP underestimates the climate effects of the
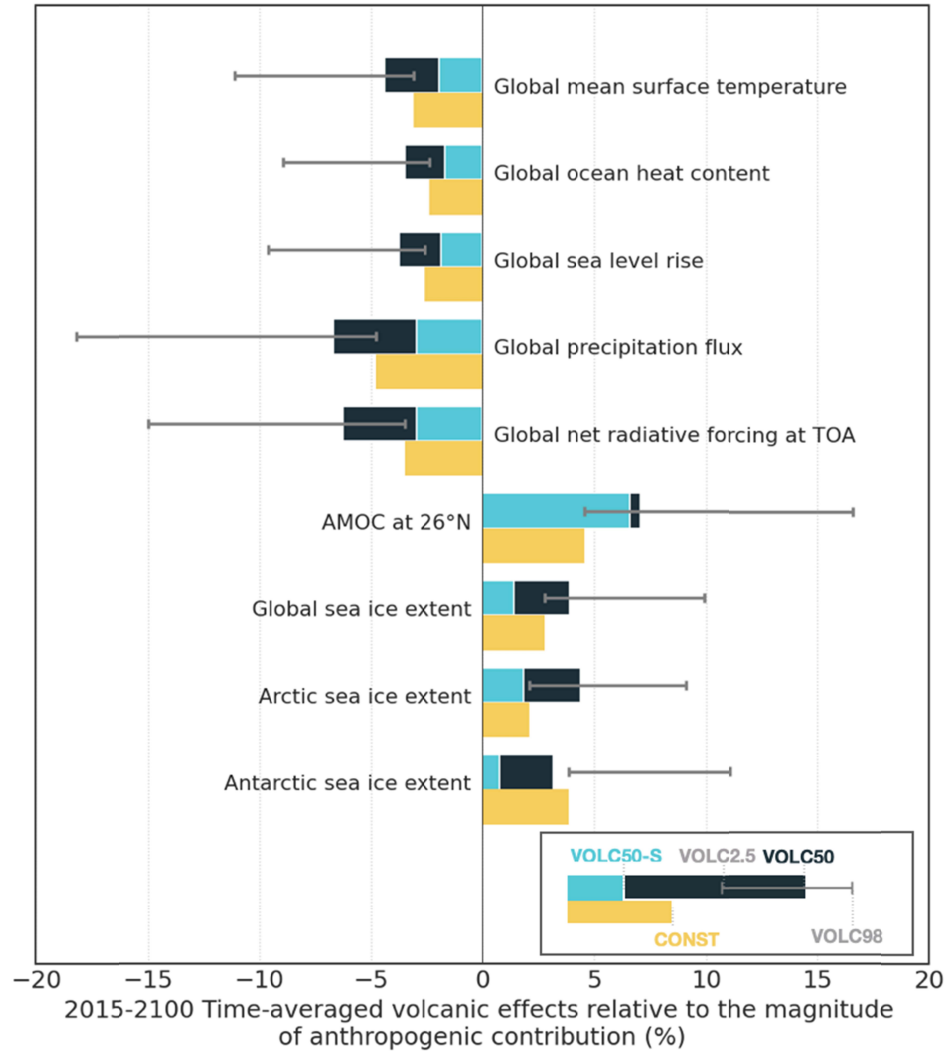311 large-scale climate indicators examined in this study.

Figure 5. Bar chart showing the time-averaged volcanic effects on large-scale climate indicators relative to the magnitude of anthropogenic contribution over the period of 2015 to 2100, i.e., VOLC50-S refers to average effects of the two VOLC50 runs with small-magnitude eruptions only.

Our simulation results show that for the SSP3-7.0 scenario, volcanic forcing can offset 2.1% to 18.2% of the anthropogenic effects to large-scale climate indicators depending on the future eruption scenarios (Figure 5). In a future scenario with low-end anthropogenic emission (SSP1-2.6), we would expect the relative effect between future volcanism and anthropogenic forcing to be much greater, e.g., by a factor of 3 for GMST since the 2015-2100 warming is 4.8 ºC in SSP3-7.0 and 1.4 ºC in SSP1-2.6. Our work highlights how the high level of uncertainty on volcanic forcing affects climate projections. For the same future eruption scenario, the volcanic effects on climate will also vary between SSP scenarios owing to climate-volcano feedbacks (e.g., Hopcroft et al., 2017; Fasullo et al., 2018; Aubry et al., 2022), which need to be quantified.

5. Conclusion

331

332   We performed climate model simulations from 2015 to 2100 with stochastic future
333 eruption scenarios using UKESM-VPLUME (a plume-aerosol-chemistry-climate model
334 framework that accounts for climate-volcano feedbacks) to examine how the uncertainties on
335 volcanic forcing affect climate projections. Using the latest ice-core and satellite datasets, we
336 show that the 2015 to 2100 volcanic SO_2 flux from explosive eruptions has a 95% probability to
337 exceed the 1850-2014 flux, which was used to derive volcanic forcing in CMIP6 ScenarioMIP.
338 Our simulations suggest that the time-averaged SAOD in a median future scenario is 0.024 (95%
339 uncertainty: 0.015-0.062), which is double that in ScenarioMIP, and that ScenarioMIP very
340 likely underestimates the future volcanic effects on climate. Our study emphasizes the
341 importance of the climate effects of future volcanic eruptions relative to the anthropogenic
342 contribution, which even for an upper end anthropogenic forcing scenario (SSP3-7.0) can range
343 between 2.1% to 18.2% for large-scale climate indicators. We also highlight the climate-
344 relevance of small-magnitude eruptions, which are responsible for 30% to 50% of the volcanic
345 effects on selected climate indicators. Future climate projection studies could either use our
346 stochastic eruption scenarios generated using state-of-the-art volcanic emission inventories, or
347 use a time-averaged constant forcing that better represents long-term volcanic activity and
348 accounts for small-magnitude eruption contributions.

349

358 **Data Availability Statement**

359 The data presented in this study are available in the University of Cambridge data repository:
360 https://doi.org/10.17863/CAM.94912. All data used for this study is with the license Creative
361 Commons Attribution 4.0 International (CC-BY-4.0).

References

Ammann, C. M., & Naveau, P. (2010). A statistical volcanic forcing scenario generator for climate simulations. *Journal of Geophysical Research: Atmospheres*, *115*(D5). https://doi.org/10.1029/2009JD012550

Archibald, A. T., O'Connor, F. M., Abraham, N. L., Archer-Nicholls, S., Chipperfield, M. P., Dalvi, M., Folberth, G. A., Dennison, F., Dhomse, S. S., Griffiths, P. T., Hardacre, C., Hewitt, A. J., Hill, R. S., Johnson, C. E., Keeble, J., Köhler, M. O., Morgenstern, O., Mulcahy, J. P., Ordóñez, C., … Zeng, G. (2020). Description and evaluation of the UKCA stratosphere–troposphere chemistry scheme (StratTrop vn 1.0) implemented in UKESM1. *Geoscientific Model Development*, *13*(3), 1223–1266. https://doi.org/10.5194/gmd-13-1223-2020

Aubry, T. J., & Jellinek, A. M. (2018). New insights on entrainment and condensation in volcanic plumes: Constraints from independent observations of explosive eruptions and implications for assessing their impacts. *Earth and Planetary Science Letters*, 490, 132-142. https://doi.org/10.1016/j.epsl.2018.03.028

Aubry, T. J., Cerminara, M., & Jellinek, A. M. (2019). Impacts of Climate Change on Volcanic Stratospheric Injections: Comparison of 1-D and 3-D Plume Model Projections. *Geophysical Research Letters*, *46*(17–18), 10609–10618. https://doi.org/10.1029/2019GL083975

Aubry, T. J., Staunton-Sykes, J., Marshall, L. R., Haywood, J., Abraham, N. L., & Schmidt, A. (2021). Climate change modulates the stratospheric volcanic sulfate aerosol lifecycle and radiative forcing from tropical eruptions. *Nature Communications*, *12*(1), 4708. https://doi.org/10.1038/s41467-021-24943-7

Aubry, T. J., Farquharson, J. I., Rowell, C. R., Watt, S. F., Pinel, V., Beckett, F., Fasullo, J., Hopcroft, P. O., Pyle, D. M., Schmidt, A., & Sykes, J. S. (2022). Impact of climate change on volcanic processes: current understanding and future challenges. *Bulletin of Volcanology*, *84*(6), 1–11. https://doi.org/10.1007/s00445-022-01562-8

Bethke, I., Outten, S., Otterå, O. H., Hawkins, E., Wagner, S., Sigl, M., & Thorne, P. (2017). Potential volcanic impacts on future climate variability. *Nature Climate Change*, *7*(11), 799–805. https://doi.org/10.1038/nclimate3394

Butchart, N. (2014). The Brewer-Dobson circulation. Reviews of geophysics, 52 (2), 157–184. https://doi.org/10.1002/2013RG000448

Carn, S. A., Clarisse, L., & Prata, A. J. (2016). Multi-decadal satellite measurements of global volcanic degassing. *Journal of Volcanology and Geothermal Research*, *311*, 99–134. https://doi.org/10.1016/j.jvolgeores.2016.01.002

407   Carn, S. (2022). *Multi-Satellite Volcanic Sulfur Dioxide L4 Long-Term Global Database*
408   *V4 (MSVOLSO2L4 4)* [Data set]. Goddard Earth Science Data and Information Services
409   Center (GES DISC). https://disc.gsfc.nasa.gov/datasets/MSVOLSO2L4_4/summary
410

411   Costa, A., Suzuki, Y. J., Cerminara, M., Devenish, B. J., Ongaro, T. E., Herzog, M., Van
412   Eaton, A. R., Denby, L., Bursik, M., Vitturi, M. d., et al. (2016). Results of the eruptive
413   column model inter-comparison study. *Journal of Volcanology and Geothermal*
414   *Research*, *326*, 2–25. https://doi.org/10.1016/j.jvolgeores.2016.01.017
415

416   Devenish, B., & Cerminara, M. (2018). The transition from eruption column to umbrella
417   cloud. *Journal of Geophysical Research: Solid Earth*, *123*(12), 10–418.
418   https://doi.org/10.1029/2018JB015841
419

420   Dhomse, S. S., Emmerson, K. M., Mann, G. W., Bellouin, N., Carslaw, K. S.,
421   Chipperfield, M. P., Hommel, R., Abraham, N. L., Telford, P., Braesicke, P., Dalvi, M.,
422   Johnson, C. E., O'Connor, F., Morgenstern, O., Pyle, J. A., Deshler, T., Zawodny, J. M.,
423   & Thomason, L. W. (2014). Aerosol microphysics simulations of the Mt. Pinatubo
424   eruption with the UM-UKCA composition-climate model. *Atmospheric Chemistry and*
425   *Physics*, *14*(20), 11221–11246. https://doi.org/10.5194/acp-14-11221-2014
426

427   Dogar, M. M., Sato, T., & Liu, F. (2020). Ocean Sensitivity to Periodic and Constant
428   Volcanism. *Scientific Reports*, *10*(1), 293. https://doi.org/10.1038/s41598-019-57027-0
429

430   Eyring, V., Bony, S., Meehl, G. A., Senior, C. A., Stevens, B., Stouffer, R. J., & Taylor,
431   K. E. (2016). Overview of the Coupled Model Intercomparison Project Phase 6 (CMIP6)
432   experimental design and organization. *Geoscientific Model Development*, *9*(5), 1937–
433   1958. https://doi.org/10.5194/gmd-9-1937-2016
434

435   Fasullo, J. T., Tilmes, S., Richter, J. H., Kravitz, B., MacMartin, D. G., Mills, M. J., &
436   Simpson, I. R. (2018). Persistent polar ocean warming in a strategically geoengineered
437   climate. *Nature Geoscience*, *11*(12), 910–914. https://doi.org/10.1038/s41561-018-0249-
438   7
439

440   Fero, J., Carey, S. N., & Merrill, J. T. (2009). Simulating the dispersal of tephra from the
441   1991 Pinatubo eruption: Implications for the formation of widespread ash layers. *Journal*
442   *of Volcanology and Geothermal Research*, *186*(1-2), 120-131.
443   https://doi.org/10.1016/j.jvolgeores.2009.03.011
444

445   Gautier, E., Savarino, J., Hoek, J., Erbland, J., Caillon, N., Hattori, S., Yoshida, N.,
446   Albalat, E., Albarede, F., & Farquhar, J. (2019). 2600-years of stratospheric volcanism
447   through sulfate isotopes. *Nature Communications*, *10*(1), 466.
448   https://doi.org/10.1038/s41467-019-08357-0
449

450   Global Volcanism Program (2022). Volcanoes of the World (v. 4.11.1; 29 Aug 2022).
451   [Database]. Distributed by Smithsonian Institution, compiled by Venzke, E.
452   https://doi.org/10.5479/si.GVP.VOTW5-2022.5.0

453

454   Guo, S., Bluth, G. J., Rose, W. I., Watson, I. M., & Prata, A. J. (2004). Re-evaluation of
455   SO2 release of the 15 June 1991 Pinatubo eruption using ultraviolet and infrared satellite
456   sensors. *Geochemistry, Geophysics, Geosystems*, 5(4).
457   https://doi.org/10.1029/2003GC000654

458

459   Hersbach, H., Bell, B., Berrisford, P., Biavati, G., Horányi, A., Muñoz Sabater, J.,
460   Nicolas, J., Peubey, C., Radu, R., Rozum, I., Schepers, D., Simmons, A., Soci, C., Dee,
461   D., Thépaut, J-N. (2019). *ERA5 monthly averaged data on pressure levels from 1979 to*
462   *present* [Data set]. Copernicus Climate Change Service (C3S) Climate Data Store (CDS).
463   doi: 10.24381/cds.6860a573

464

465   Hopcroft, P. O., Kandlbauer, J., Valdes, P. J., & Sparks, R. S. J. (2018). Reduced cooling
466   following future volcanic eruptions. *Climate Dynamics*, *51*(4), 1449–1463.
467   https://doi.org/10.1007/s00382-017-3964-7

468

469   IPCC, 2021: Climate Change 2021: The Physical Science Basis. Contribution of Working
470   Group I to the Sixth Assessment Report of the Intergovernmental Panel on Climate
471   Change [Masson-Delmotte, V., P. Zhai, A. Pirani, S.L. Connors, C. Péan, S. Berger, N.
472   Caud, Y. Chen, L. Goldfarb, M.I. Gomis, M. Huang, K. Leitzell, E. Lonnoy, J.B.R.
473   Matthews, T.K. Maycock, T. Waterfield, O. Yelekçi, R. Yu, and B. Zhou (eds.)].
474   Cambridge University Press, Cambridge, United Kingdom and New York, NY, USA, In
475   press, doi:10.1017/9781009157896.

476

477   Kalnay, E., Kanamitsu, M., Kistler, R., Collins, W., Deaven, D., Gandin, L., Iredell, M.,
478   Saha, S., White, G., Woollen, J., Zhu, Y., Chelliah, M., Ebisuzaki, W., Higgins, W.,
479   Janowiak, J., Mo, K. C., Ropelewski, C., Wang, J., Leetmaa, A., Reynolds, R., Jenne, R.,
480   & Joseph, D. (1996). The NCEP/NCAR 40-Year Reanalysis Project, *Bulletin of the*
481   *American Meteorological Society*, *77*(3), 437–472. https://doi.org/10.1175/1520-
482   0477(1996)077<0437:TNYRP>2.0.CO;2

483

484   Marshall, L. R., Maters, E. C., Schmidt, A., Timmreck, C., Robock, A., & Toohey, M.
485   (2022). Volcanic effects on climate: recent advances and future avenues. *Bulletin of*
486   *Volcanology*, *84*(5), 1–14. https://doi.org/10.1007/s00445-022-01559-3

487

488   Mastin, L. G. (2007). A user-friendly one-dimensional model for wet volcanic plumes.
489   *Geochemistry, Geophysics, Geosystems*, *8*(3). https://doi.org/10.1029/2006GC001455

490

491   Mastin, L. G. (2014). Testing the accuracy of a 1-D volcanic plume model in estimating
492   mass eruption rate. *Journal of Geophysical Research: Atmospheres*, *119*(5), 2474–2495.
493   https://doi.org/10.1002/2013JD020604

494

495   Mastrandrea, M. D., Field, C. B., Stocker, T. F., Edenhofer, O., Ebi, K. L., Frame, D. J.,
496   Held, H., Kriegler, E., Mach, K. J., Matschoss, P. R., Plattner, G. K. (2010). Guidance
497   note for lead authors of the IPCC fifth assessment report on consistent treatment of
498   uncertainties. https://

499   www.ipcc.ch/site/assets/uploads/2017/08/AR5_Uncertainty_Guidance_Note.pdf

500

501   McCormick, M. P., Thomason, L. W., & Trepte, C. R. (1995). Atmospheric effects of the
502   Mt Pinatubo eruption. *Nature*, *373*(6513), 399–404. https://doi.org/10.1038/373399a0

503

504   Neely III, R.R. & Schmidt, A. (2016). *VolcanEESM: Global volcanic sulphur dioxide*
505   *(SO2) emissions database from 1850 to present - Version 1.0* [Data set]. Centre for
506   Environmental Data Analysis. http://dx.doi.org/10.5285/76ebdc0b-0eed-4f70-b89e-
507   55e606bcd568

508

509   O'Neill, B. C., Tebaldi, C., van Vuuren, D. P., Eyring, V., Friedlingstein, P., Hurtt, G.,
510   Knutti, R., Kriegler, E., Lamarque, J.-F., Lowe, J., Meehl, G. A., Moss, R., Riahi, K., &
511   Sanderson, B. M. (2016). The Scenario Model Intercomparison Project (ScenarioMIP)
512   for CMIP6. *Geoscientific Model Development*, *9*(9), 3461–3482.
513   https://doi.org/10.5194/gmd-9-3461-2016

514

515   Pausata, F. S. R., Chafik, L., Caballero, R., & Battisti, D. S. (2015). Impacts of high-
516   latitude volcanic eruptions on ENSO and AMOC. *Proceedings of the National Academy*
517   *of Sciences*, *112*(45), 13784–13788. https://doi.org/10.1073/pnas.1509153112

518

519   Santer, B. D., Bonfils, C., Painter, J. F., Zelinka, M. D., Mears, C., Solomon, S., Schmidt,
520   G. A., Fyfe, J. C., Cole, J. N. S., Nazarenko, L., Taylor, K. E., & Wentz, F. J. (2014).
521   Volcanic contribution to decadal changes in tropospheric temperature. *Nature*
522   *Geoscience*, *7*(3), 185–189. https://doi.org/10.1038/ngeo2098

523

524   Schmidt, A., Mills, M. J., Ghan, S., Gregory, J. M., Allan, R. P., Andrews, T., Bardeen,
525   C. G., Conley, A., Forster, P. M., Gettelman, A., Portmann, R. W., Solomon, S., & Toon,
526   O. B. (2018). Volcanic Radiative Forcing From 1979 to 2015. *Journal of Geophysical*
527   *Research: Atmospheres*, *123*(22), 12491–12508. https://doi.org/10.1029/2018JD028776

528

529   Mulcahy, J. P., Jones, C. G., Rumbold, S. T., Kuhlbrodt, T., Dittus, A. J., Blockley, E.
530   W., Yool, A., Walton, J., Hardacre, C., Andrews, T., Bodas-Salcedo, A., Stringer, M., de
531   Mora, L., Harris, P., Hill, R., Kelley, D., Robertson, E., & Tang, Y. (2023). UKESM1.1:
532   Development and evaluation of an updated configuration of the UK Earth System Model.
533   *Geoscientific Model Development Discussions*, in press. https://doi.org/10.5194/gmd-
534   2022-113

535

536   Sigl, M., Toohey, M., McConnell, J. R., Cole-Dai, J., & Severi, M. (2022). Volcanic
537   stratospheric sulfur injections and aerosol optical depth during the Holocene (past 11 500
538   years) from a bipolar ice-core array. *Earth System Science Data*, *14*(7), 3167–3196.
539   https://doi.org/10.5194/essd-14-3167-2022

540

541   Sigl, M., Winstrup, M., McConnell, J. R., Welten, K. C., Plunkett, G., Ludlow, F.,
542   Büntgen, U., Caffee, M., Chellman, N., Dahl-Jensen, D., Fischer, H., Kipfstuhl, S.,
543   Kostick, C., Maselli, O. J., Mekhaldi, F., Mulvaney, R., Muscheler, R., Pasteris, D. R.,
544   Pilcher, J. R., … Woodruff, T. E. (2015). Timing and climate forcing of volcanic

545   eruptions for the past 2,500 years. *Nature*, *523*(7562), 543–549.
546   https://doi.org/10.1038/nature14565

547

548   Stoffel, M., Khodri, M., Corona, C., Guillet, S., Poulain, V., Bekki, S., Guiot, J.,
549   Luckman, B. H., Oppenheimer, C., Lebas, N., Beniston, M., & Masson-Delmotte, V.
550   (2015). Estimates of volcanic-induced cooling in the Northern Hemisphere over the past
551   1,500 years. *Nature Geoscience*, *8*(10). https://doi.org/10.1038/ngeo2526

552

553   Timmreck, C., Mann, G. W., Aquila, V., Hommel, R., Lee, L. A., Schmidt, A., Brühl, C.,
554   Carn, S., Chin, M., Dhomse, S. S., Diehl, T., English, J. M., Mills, M. J., Neely, R.,
555   Sheng, J., Toohey, M., & Weisenstein, D. (2018). The Interactive Stratospheric Aerosol
556   Model Intercomparison Project (ISA-MIP): Motivation and experimental design.
557   *Geoscientific Model Development*, *11*(7), 2581–2608. https://doi.org/10.5194/gmd-11-
558   2581-2018

559

560   Zambri, B., Robock, A., Mills, M. J., & Schmidt, A. (2019). Modeling the 1783–1784
561   Laki Eruption in Iceland: 2. Climate Impacts. *Journal of Geophysical Research:*
562   *Atmospheres*, *124*(13), 6770–6790. https://doi.org/10.1029/2018JD029554